ELSEVIER

Nuclear Instruments and Methods in Physics Research A 485 (2002) 753–767

NUCLEAR INSTRUMENTS & METHODS IN PHYSICS RESEARCH Section A

www.elsevier.com/locate/nima

Perturbed γ–γ correlations from oriented nuclei and static moment measurements I: formalism and principles

Andrew E. Stuchbery*, Martyn P. Robinson

Department of Nuclear Physics, Research School of Physical Sciences and Engineering, The Australian National University, Canberra, ACT 0200, Australia

Received 9 August 2001; accepted 21 August 2001

Abstract

A formalism to interpret the perturbations of γ–γ directional correlations from nuclei oriented by heavy-ion induced reactions is described. Applications to multidetector arrays are considered and aspects of experiments designed to measure magnetic dipole moments of excited nuclear states are considered.

PACS: 23.20.En; 21.10.Ky; 29.30.Kv

Keywords: Perturbed directional correlations from oriented nuclei; DCO; Nuclear moments; *g* factors

1. Introduction

Directional correlations of coincident γ-rays emitted from reaction-oriented nuclei are frequently used in the analysis of data obtained from multidetector arrays to determine the multipolarities of γ-rays and hence the spins and parities of the nuclear levels that they connect [1–5]. The abbreviation DCO (directional correlations from oriented nuclei) is frequently used when there is an aligned initial state followed by an angular correlation between the de-excitation radiations.

If an atomic nucleus is subjected to a sufficiently strong magnetic field, or an electric field gradient, the orientation of its spin will change and the directional correlations of the γ-rays that it emits will be perturbed [6–9]. The magnitude of the perturbation depends on the size of the local field and on the properties of the nucleus. The interest here is in measuring and interpreting such *perturbed* directional correlations with a view to extracting the magnetic dipole moment or the electric quadrupole moment of an excited nuclear state.

While perturbed angular correlations and perturbed angular distributions have been exploited for many years to study nuclei and the hyperfine fields that surround them in a variety of media [6–9], perturbed directional correlations from oriented nuclei, or equivalently perturbed triple (or higher fold) correlations, have hardly been exploited at all.

*Corresponding author. Tel.: +61-2-6125-2097; fax: +61-2-6125-0748.

E-mail address: andrew.stuchbery@anu.edu.au (A.E. Stuchbery).

0168-9002/01/$ - see front matter
PII: S0168-9002(01)02114-3

With the increasing power and availability of large arrays of γ-ray detectors, this situation is changing. There have been several measurements in recent years that use arrays to measure magnetic moments of excited nuclear states [10–19]. While some of these measurements used radioactive decay to populate the states of interest — and hence the standard angular correlation formalism — others were in-beam measurements that analyzed the data *approximately* in terms of the simpler perturbed angular distribution formalism [15–17]. A few measurements have used perturbed directional correlations from reaction-oriented nuclei in the geometry where the magnetic field is along the beam direction [18,19]. In this special case, the formalism reduces to a simple form that is much like that for perturbed angular correlations (see below). There is a clear need, however, to develop the perturbed directional correlation formalism rigorously for more general applications to perturbed correlation measurements in multidetector arrays.

A number of advantages ensue from employing multidetector arrays and coincidence techniques to measure static electric and magnetic moments of excited nuclear states, especially in unstable nuclei populated by heavy-ion reactions. Aside from the improved peak-to-background obtained in coincidence γ-ray spectra, the coincidence requirement also enables the separation of the perturbation that takes place in the level of interest from the perturbations of the levels that feed it (which are nearly always present when the states of interest are populated in fusion-evaporation reactions).

The present paper describes the formalism required to interpret perturbed γ–γ directional correlations from reaction-oriented nuclei and gives some hypothetical examples of a pedagogical nature that serve to guide the design of experiments. We will focus here on the development of the general formalism and apply it to magnetic perturbations. The effects of combined electric quadrupole and magnetic dipole interactions and their application to extract nuclear quadrupole moments will be described elsewhere [20]. The first applications of the formalism to data taken with the Australian National University array CAESAR are presented in an accompanying paper [21] and elsewhere [22].

2. Formalism

2.1. General experimental considerations

For the present purposes, it will be assumed that the nuclei of interest are populated in a heavy-ion fusion-evaporation reaction and that they are somehow exposed to external electric and/or magnetic fields that perturb the orientation of the nuclear spin. At first, to keep the formalism general, the perturbing field will not be specified. Specific perturbations will be considered in Section 2.6. It will also be assumed that the nuclei of interest are populated at high excitation energy and spin and that they decay by a sequence of γ-ray transitions in cascade. Some of these de-excitation γ-rays are observed in coincidence using a multidetector array. There may be some transitions in the cascade that are not observed, and in principle, there can be any number of detectors that fire in the event (i.e. any fold). After considering the formalism applicable for any fold, we will focus on the case of two-fold events and illustrate the effects of various magnetic perturbations.

2.2. Notation and relation to previous work

In the following subsections, the general formulae are summarized from which the perturbed directional correlation function can be calculated for any of the situations of interest. Discussion will be limited to nuclei that are aligned (but not polarized) by the reaction mechanism and the polarization of the emitted γ-rays will not be detected. Beyond that, the formulae that are required to evaluate the correlation function for any cascade of states and any fold of coincidence data with no restriction on the detection angles or field orientation will be given.

The coordinate frame employed here is always that in which the beam is directed along the positive z-axis and the formalism used is essentially that of Alder and Winther [23]. However we do not normalize the statistical tensors (as they do) because this removes information that is required to calculate the DCOs for all detector combinations in a multidetector array in such a way that they can be compared consistently on an equal footing, for example in a global fit to the whole data set. It can be noted that the expressions for unperturbed DCOs given by Krane et al. [1] follow from the present formulae provided that the statistical tensors of the intermediate state are *not* normalized.

The present formulation is based on expressions given by Alder and Winther [23], which are also presented (with a few changes in notation) by Steffen and Alder in Ref. [7]. However, as far as possible we will use, or at least make connections with, the notations of Krane et al. [1], and Yamazaki [24], which are commonly used by those who work with γ-ray detector arrays [2–5].

Our work took inspiration from the report of Ward et al. [25] which considered angular correlations in the 8π array. While the present work was in progress, we became aware of the work of Furuno in relation to perturbed angular correlations in the UTTAC crystal ball [26]. We are not aware of any other work on the perturbed DCO formalism for a multidetector array. The previous work, which appears in laboratory reports, is not as general as the present work aims to be. In particular, the previous work [18,25,26] has focused upon the case where a magnetic field is directed along the beam direction. This leads to a much simplified perturbation function that has a form like the familiar perturbed angular correlation (see below, Section 3.2). We are interested in a more general formulation that allows magnetic and electric perturbations due to fields in any direction with respect to the beam, and specific applications to the case where the magnetic field is perpendicular to the beam. The merits of alternative field directions with respect to the detector locations and the beam axis will be discussed in Section 3.

2.3. Unperturbed DCOs

Fig. 1 shows the notation used to label the levels in a cascade of interest. The initial state of interest populated by the reaction (or by previously emitted unobserved γ-ray cascades above the state of interest) is denoted as I_1. Its alignment is specified by a statistical tensor [23] denoted as $\rho_{k_1q_1}(I_1)$, where $q_1 = 0$ for the initial state, which is related to the statistical tensor often denoted as $B_{k_1}(I_1)$ [8] by

$$\rho_{k_1q_1}(I_1) = \delta_{q_10}B_{k_1}(I_1)/\sqrt{2k_1+1} \tag{1}$$

and

$$B_{k_1}(I_1) = \sqrt{2I_1+1}\sum_m(-)^{I_1+m} \langle I_1 - mI_1m \,|\, k_10\rangle P_m \tag{2}$$

where P_m specifies the m-substate population distribution and δ_{q_10} is the Kronecker delta symbol. $k_1 = 0, 2, 4, \ldots 2I_1$ if I_1 is an integer, and $k_1 = 0, 2, 4, \ldots 2I_1 - 1$ if I_1 is half-integer. P_m is often approximated by a Gaussian distribution [24]:

$$P_m = \frac{\exp(-m^2/2\sigma^2)}{\sum_{m'=-I_1}^{I_1}\exp(-m'^2/2\sigma^2)} \tag{3}$$

where, typically, the parameter $\sigma/I \approx 0.3$ for heavy nuclei populated following heavy-ion induced fusion-evaporation reactions [27].

We now consider that the state I_1 decays to state I_2 by the emission of a γ-ray with multipolarities L and L'. If the γ-ray is observed in a detector at the spherical polar angles θ_1 and ϕ_1 (in the coordinate frame where the z-axis is the beam axis), the statistical tensor of the state I_2 becomes:

$$\begin{aligned}\rho_{k_2q_2}(I_2) = &\sum_{k,q,k_1,q_1}\rho_{k_1q_1}(I_1)(-1)^{k_1+q_1} \\ &\times\sqrt{\frac{(2k+1)(2k_1+1)}{(2k_2+1)}}\begin{pmatrix} k_1 & k & k_2 \\ -q_1 & q & q_2\end{pmatrix} \\ &\times A_k^{k_2k_1}(\delta_{\gamma_{12}}LL'I_2I_1)Q_k(E_{\gamma_{12}})D_{q0}^{k*}(\phi_1,\theta_1,0)\end{aligned} \tag{4}$$

where $k_2 = 0, 2, 4, \ldots, 2I_2$ if I_2 is an integer, and $k_2 = 0, 2, 4, \ldots, 2I_2 - 1$ if I_2 is half-integer; $k = 0, 2, 4, \ldots, 2L_{\max}$, where $L_{\max}$ is the larger of L and L'. $q = -k, -k+1, -k+2, \ldots, 0, 1, 2, \ldots, k$. ($q_1$ and q_2 are likewise related to k_1 and k_2.) The quantity $Q_k(E_{\gamma_{12}})$ is the solid-angle attenuation coefficient which takes account of the finite solid-angle opening of the γ-ray detector [28–30] and

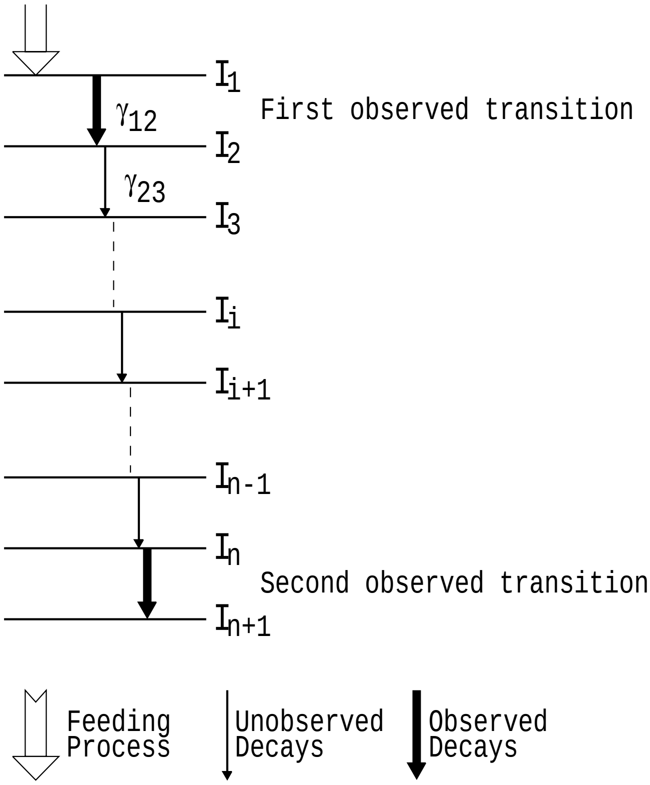

Fig. 1. Notation used to label levels in a general cascade.

$D^k_{q0}(\phi,\theta,0)$ is the rotation matrix [23]. $A_k^{k_2k_1}(\delta_{\gamma_{12}}LL'I_2I_1)$ is related to the so-called generalized F-coefficient for the γ-ray transition between the states I_1 and I_2 with mixed multipolarities L and L' and mixing ratio $\delta_{\gamma_{12}}$ [1,23] by the expression:

$$A_k^{k_2k_1}(\delta LL'I_2I_1) = [F_k^{k_2k_1}(LLI_2I_1) + 2\delta F_k^{k_2k_1}(LL'I_2I_1) + \delta^2 F_k^{k_2k_1}(L'L'I_2I_1)]/(1+\delta^2). \tag{5}$$

It is worth noting that the F-coefficients vanish unless a number of 'triangle' conditions are satisfied. In addition to the ranges of k, k_1 and k_2 noted above, we also have the conditions that

$$|L-L'| \leqslant k \leqslant L+L' \tag{6}$$

and

$$|k_1-k_2| \leqslant k \leqslant k_1+k_2. \tag{7}$$

This means that if we are considering a cascade in which the highest multipolarity is $L=2$, i.e. quadrupole radiation, then $k=0,2,4$ only. Furthermore, since $k_2=0,2,4$ also in this case (see below), then $k_1 \leqslant 8$. Recognition of this saves considerable computation, especially for high-spin states.

If the γ-ray is not observed, the statistical tensor $\rho_{k_2q_2}(I_2)$ may be evaluated by taking $k=0$ only in Eq. (4); it then reduces to the familiar form

$$\rho_{k_2q_2}(I_2) = U_{k_1}(\delta_{\gamma_{12}}LL'I_2I_1)\ \delta_{k_1k_2}\delta_{q_1q_2}\rho_{k_1q_1}(I_1) \tag{8}$$

where

$$U_k(\delta LL'I_2I_1) = [U_k(LI_2I_1) + \delta^2 U_k(L'I_2I_1)]/(1+\delta^2) \tag{9}$$

and the U-coefficients are as in Refs. [8,24], for example.

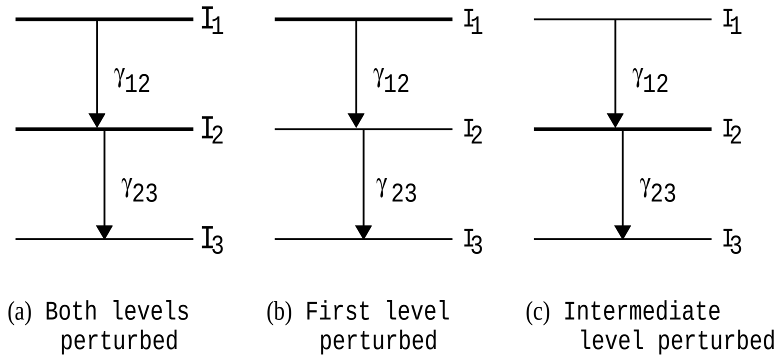

Fig. 2. The three level cascade: (a) General case where both I_1 and I_2 are perturbed. (b) Only the first level, I_1, is perturbed. (c) Only the intermediate state, I_2, is perturbed.

Eq. (4) may be applied iteratively to propagate the statistical tensor along a cascade of any length, whether any individual transition is observed or not, until the final state of interest is reached. For convenience here we will generally consider a two-fold coincidence for the three-level sequence $I_1 \to I_2 \to I_3$ with no unobserved intermediate transitions, as shown in Fig. 2, since more general cases simply require repeated application of the expressions given above.

The intensity of the γ-ray transition $I_2 \to I_3$ observed in a detector at polar angles (θ_2, ϕ_2), is determined from the statistical tensor of the state I_2 using the expression

$$W = \sum_{k_2,q_2} \rho_{k_2q_2}(I_2)\sqrt{(2k_2+1)}A_{k_2}(\delta_{\gamma_{23}}LL'I_3I_2) \times Q_{k_2}(E_{\gamma_{23}})D^{k_2\,*}_{q_20}(\phi_2,\theta_2,0) \quad (10)$$

where $A_{k_2}(\delta_{\gamma_{23}}LL'I_3I_2)$ is related to the 'ordinary' F-coefficients [1,8,24] by an expression of the same form as Eq. (5). The 'ordinary' F-coefficients are a special case of the generalized F-coefficient,

$$F_k(L,L',I_2,I_1) = F_k^{0,k}(L,L',I_2,I_1) = (-1)^{L+L'}F_k^{k,0}(L,L',I_1,I_2). \quad (11)$$

(The remaining quantities in Eq. (10) are as defined for Eq. (4).) It can be seen that for a cascade where L and L' are not greater than 2, the triangle conditions on the F coefficient require that $0 \leqslant k_2 \leqslant 4$.

We now have the expressions required to evaluate the unperturbed DCO for any general cascade of any fold. Furthermore, if Eqs. (1), (4) and (10) are combined for the case of $I_1 \to I_2 \to I_3$, the result is an expression that is equivalent to the expressions given in Eqs. (9)–(12) of the paper by Krane et al. [1].

2.4. Perturbed DCOs: general considerations

Alder and Winther [23] write the perturbation of the statistical tensor for state I due to extranuclear fields that act on the nucleus from time zero until time t as

$$\rho_{k'q'}(I,t) = \sum_{k,q} \rho_{kq}(I,t=0)[G^{qq'}_{kk'}(t)]^* \sqrt{\frac{(2k+1)}{(2k'+1)}} \quad (12)$$

where $G^{qq'}_{kk'}(t)$ is the time-dependent perturbation factor. The perturbation may allow k and k' to take both even and odd values, however only even values are relevant here because the reactions of interest do not introduce polarization and the polarization of the γ-rays is not detected. The relation between the perturbation factor and its complex conjugate is

$$[G^{qq'}_{kk'}(t)]^* = (-1)^{q-q'}G^{-q-q'}_{kk'}(t). \quad (13)$$

Often the expressions for the perturbations due to external fields are given in a co-ordinate frame where the field is along the z-axis, whereas the expressions for the angular correlations considered here are for a frame with the beam along the

z-axis. It is necessary therefore to transform the perturbation factors into the correct frame. If the Euler angles (α, β, γ) specify the rotation required to transform the 'beam' frame into the 'field' frame,[1] then

$$[G_{kk'}^{qq'}(t)]^* = \sum_{Q,Q'} D_{qQ}^{k\,*}(\alpha,\beta,\gamma)[\mathcal{G}_{kk'}^{QQ'}(t)]^* D_{q'Q'}^{k'}(\alpha,\beta,\gamma)$$
$$= \sum_{Q,Q'} (-1)^{q-Q} D_{-q-Q}^{k}(\alpha,\beta,\gamma)[\mathcal{G}_{kk'}^{QQ'}(t)]^* \times D_{q'Q'}^{k'}(\alpha,\beta,\gamma) \quad (14)$$

where $[\mathcal{G}_{kk'}^{QQ'}(t)]^*$ is the perturbation factor in the 'field' frame.

We now have the formalism required to calculate the perturbed DCO (PDCO), at least in principle, for any case of interest. For the formulation of the general problem it remains to show the formulae required to obtain the ensemble time average of the perturbations along a sequence of decays.

Consider a sequence of $n+1$ levels in cascade like that in Fig. 1, all subject to perturbations from the time of their population until they decay. We want the PDCO function corresponding to the detection of a coincidence between the transitions $I_1 \rightarrow I_2$ and $I_n \rightarrow I_{n+1}$. If the first level I_1 is populated at $t=0$ and decays at time t_1 to the second level I_2, which decays at time t_2, etc., then we denote the PDCO function as

$$W(t_1, t_2, \ldots, t_n) = W(G^*(I_1, t_1), G^*(I_2, t_2 - t_1), \ldots, G^*(I_n, t_n - t_{n-1})) \quad (15)$$

to indicate that the time dependence enters through the time-dependent perturbation factors for the states I_i, $G^*(I_i, t)$. To make comparisons with experiment, the times t_i at which states I_i decay have to be averaged over all allowed values, i.e. from $t_i = 0$ until $t_i = t_{i+1}$. The general problem involves solving a set of nested integrals (cf. Ref. [31]). For the time-differential PDCO for the case in Fig. 1 we put $t_n = t$ and have

$$\frac{\mathrm{d}\langle W(t)\rangle}{\mathrm{d}t} = \lambda_1\lambda_2\ldots\lambda_n \int_{t_{n-1}=0}^{t} \cdots \int_{t_2=0}^{t_3} \int_{t_1=0}^{t_2} W(t_1, t_2, \ldots, t) \times \mathrm{e}^{-\lambda_1 t_1}\mathrm{e}^{-\lambda_2(t_2-t_1)}\cdots\mathrm{e}^{-\lambda_n(t-t_{n-1})}\,\mathrm{d}t_1\,\mathrm{d}t_2\ldots\mathrm{d}t_{n-1} \quad (16)$$

where $\lambda_i = 1/\tau_i$ is the decay rate for state I_i and τ_i is its meanlife. The time-integral correlation is then evaluated as

$$\langle W\rangle = \int_{t=0}^{\infty} \frac{\mathrm{d}\langle W(t)\rangle}{\mathrm{d}t}\,\mathrm{d}t. \quad (17)$$

It is neither possible nor profitable to attempt to deal further with a completely general formulation. We will therefore proceed by choosing some specific cases of interest.

2.5. The three-level cascade

As foreshadowed above, we now consider the special case of a two-fold coincidence for the three-level sequence $I_1 \rightarrow I_2 \rightarrow I_3$ with no unobserved intermediate transitions, as shown in Fig. 2. Along with the pedagogical value, we anticipate that in very many situations these expressions will be all that is required for the analysis of experimental data. Therefore, following the expression for the case where both I_1 and I_2 are perturbed, we also give explicit expressions for: (i) the case where only I_1 is perturbed, and (ii) the case where only I_2 is perturbed. (See Fig. 2.)

Following the formulation introduced above, the first level I_1 is populated at $t=0$ and decays at time t_1 to the second level I_2, which decays at time t, the general PDCO function is then

$$W(t_1, t) = \sum_{kk_1k_1'k_2k_2'qq_1'q_2q_2'} B_{k_1}(I_1) G_{k_1k_1'}^{0q_1'\,*}(I_1, t_1) \times G_{k_2k_2'}^{q_2q_2'\,*}(I_2, t - t_1) A_k^{k_2k_1'}(\delta_{\gamma_{12}} LL' I_2 I_1) \times A_{k_2'}(\delta_{\gamma_{23}} LL' I_3 I_2) Q_k(E_{\gamma_{12}}) Q_{k_2'}(E_{\gamma_{23}}) \times (-)^{k_1'+q_1'}\sqrt{(2k+1)} \begin{pmatrix} k_1' & k & k_2 \\ -q_1' & q & q_2 \end{pmatrix} \times D_{q0}^{k\,*}(\phi_1, \theta_1, 0) D_{q_2'0}^{k_2'\,*}(\phi_2, \theta_2, 0). \quad (18)$$

[1] The convention for the Euler angles used is: α is the first rotation about the z-axis, β is the second rotation about the new y-axis, γ is the third rotation about the new z-axis. The D matrices are as defined in Ref. [23].

For the time-differential PDCO, we have to perform the integration over t_1 to get

$$\frac{\mathrm{d}\langle W(t)\rangle}{\mathrm{d}t} = \lambda_1\lambda_2 \int_{t_1=0}^{t} W(t_1,t)\mathrm{e}^{-\lambda_1 t_1}\mathrm{e}^{-\lambda_2(t-t_1)}\,\mathrm{d}t_1 \tag{19}$$

$$= \lambda_1\lambda_2\mathrm{e}^{-\lambda_2 t} \int_{t_1=0}^{t} W(t_1,t)\mathrm{e}^{-(\lambda_1-\lambda_2)t_1}\,\mathrm{d}t_1 \tag{20}$$

where the second expression makes it clear that the perturbation is superimposed on the exponential decay of the intermediate state, I_2. The time-integral PDCO is

$$\langle W\rangle = \lambda_1\lambda_2 \int_{t=0}^{\infty}\int_{t_1=0}^{t} W(t_1,t)\mathrm{e}^{-\lambda_1 t_1} \times \mathrm{e}^{-\lambda_2(t-t_1)}\,\mathrm{d}t_1\,\mathrm{d}t. \tag{21}$$

We now write down the PDCO functions for two special cases, since in many applications only one relatively long-lived level will experience a significant perturbation while all other levels will be so short lived that the perturbations can be neglected:

(i) If only the first level I_1 is perturbed, Fig. 2(b), Eq. (18) becomes

$$\begin{aligned} W(t) = \sum_{kk_1k_1'k_2qq_1'q_2} & B_{k_1}(I_1)G_{k_1k_1'}^{0q_1'\,*}(I_1,t) \\ & \times A_k^{k_2k_1'}(\delta_{\gamma_{12}}LL'I_2I_1)A_{k_2}(\delta_{\gamma_{23}}LL'I_3I_2) \\ & \times Q_k(E_{\gamma_{12}})Q_{k_2}(E_{\gamma_{23}}) \\ & \times (-1)^{k_1'+q_1'}\sqrt{(2k+1)}\begin{pmatrix} k_1' & k & k_2 \\ -q_1' & q & q_2 \end{pmatrix} \\ & \times D_{q0}^{k\,*}(\phi_1,\theta_1,0)D_{q_20}^{k_2\,*}(\phi_2,\theta_2,0). \end{aligned} \tag{22}$$

(ii) If only the intermediate level I_2 is perturbed, Fig. 2(c), Eq. (18) becomes

$$\begin{aligned} W(t) = \sum_{kk_1k_2k_2'qq_2q_2'} & B_{k_1}(I_1)A_k^{k_2k_1}(\delta_{\gamma_{12}}LL'I_2I_1) \\ & \times G_{k_2k_2'}^{q_2q_2'\,*}(t)A_{k_2'}(\delta_{\gamma_{23}}LL'I_3I_2) \\ & \times Q_k(E_{\gamma_{12}})Q_{k_2'}(E_{\gamma_{23}}) \\ & \times (-1)^{k_1}\sqrt{(2k+1)}\begin{pmatrix} k_1 & k & k_2 \\ 0 & q & q_2 \end{pmatrix} \\ & \times D_{q0}^{k\,*}(\phi_1,\theta_1,0)D_{q_2'0}^{k_2'\,*}(\phi_2,\theta_2,0). \end{aligned} \tag{23}$$

This expression is equivalent to Eq. (1) in Furuno's report [26]. It will be used below to evaluate the PDCO in the case where a magnetic field is applied along the beam direction.

2.6. Perturbation factors

We now consider the perturbation factors for the different types of interaction. At the present time we are mainly interested in two cases: (i) pure magnetic interactions, and (ii) combined magnetic and electric interactions. Clearly either pure magnetic or pure electric interactions are a special case of the combined interaction. The pure magnetic interaction is worth considering on its own, however, because it has wide applications and is relatively simple.

A magnetic dipole interaction always causes a rotation of the angular correlation pattern about the magnetic field direction, leading to the well known "lighthouse" effect in time-differential measurements and, for time-integral measurements, a combined angular shift and attenuation of the anisotropy [6–8].

In the frame where the magnetic field is along the z-axis, the time-differential perturbation factor due to a static magnetic field B is

$$G_{kk'}^{qq'\,*}(I,t) = \delta_{qq'}\delta_{kk'}\mathrm{e}^{\mathrm{i}q\omega t} \tag{24}$$

where

$$\omega = -g\frac{\mu_\mathrm{N}}{\hbar}B \tag{25}$$

is the Lamor frequency, g is the nuclear g factor and B is the magnetic field strength.

If the field is present throughout the lifetime of the nuclear state, the integral perturbation factor is

$$G_{kk'}^{qq'\,*}(\infty) = \delta_{qq'}\delta_{kk'}\lambda\int_0^{\infty}\mathrm{e}^{-(\lambda-\mathrm{i}q\omega)t}\,\mathrm{d}t \tag{26}$$

$$= \delta_{qq'}\delta_{kk'}\frac{1}{1-\mathrm{i}q\omega\tau} \tag{27}$$

$$= \delta_{qq'}\delta_{kk'}\frac{1+\mathrm{i}q\omega\tau}{1+(q\omega\tau)^2} \tag{28}$$

$$= \delta_{qq'}\delta_{kk'}\frac{\mathrm{e}^{\mathrm{i}q\Delta\theta_q}}{\sqrt{1+(q\omega\tau)^2}} \tag{29}$$

where

$$\tan(q\Delta\theta_q) = q\omega\tau. \tag{30}$$

Thus when the precession angle $\omega\tau$ is large there is both a rotation and an attenuation of the radiation pattern. For small $\omega\tau$, however,

$$G_{kk}^{qq*}(\infty) \approx e^{iq\omega\tau} \tag{31}$$

and the integral perturbation is a pure rotation about the field direction.

In the case of the transient field [32], which acts for only about a picosecond or thereabouts while the nucleus is moving within a ferromagnetic medium, the integral perturbation factor is

$$G_{kk}^{qq*}(\infty) = \int_0^T G_{kk}^{qq*}(t)e^{-t/\tau}(dt/\tau) + G_{kk}^{qq*}(T)e^{-T/\tau} \tag{32}$$

where T is the time for which the transient field acts. Provided $\tau \gg T$, then

$$G_{kk}^{qq*}(\infty) \approx G_{kk}^{qq*}(T) = e^{iq\Delta\theta_{tf}} \tag{33}$$

where

$$\Delta\theta_{tf} = g\frac{\mu_N}{\hbar}\int_0^T B_{tr}(t)\, dt. \tag{34}$$

The perturbation due to the transient field can therefore be treated as a small rotation about the field direction. Clearly, small precessions, like the transient field effect, can be treated as a shift in the effective detection angle about the applied field direction without resorting to the full PDCO formalism.

Along with pure magnetic interactions, we are also interested in the combined effect of magnetic dipole and electric quadrupole interactions, particularly for impurity nuclei in gadolinium hosts. To treat this case, we have adapted the formalism of Alder et al. [33,34]. This situation will be discussed in greater detail elsewhere [20]. To keep the discussion focused here, only pure magnetic interactions are considered in the examples that follow.

3. Examples of magnetic perturbations

3.1. General comments

Our initial aim was to employ the PDCO formalism to measure g factors of states with lifetimes sufficiently long as to produce 'healthy' integral precession angles, $\omega\tau$, of the order of 100–500 mrad through interactions of the nuclear moment with the static hyperfine magnetic field. This provides the context for the following discussion.

Usually, the locations of detectors in multi-detector arrays are chosen and fixed on grounds other than for optimal perturbed angular correlation measurements. For some arrays there may be some choice of the magnetic field direction with respect to the beam direction and the detection angles, but in many cases there is little choice. In general, for optimal perturbed angular correlation/distribution measurements, the detectors should be either in — or near — the plane perpendicular to the magnetic field direction and should be located at symmetric angles with respect to the beam axis [8,9,32].

3.2. Field along the beam direction

Putting the magnetic field along the beam direction has the great advantage of simplifying the effect of the perturbation. Because the reaction aligns the nuclei symmetrically about the beam axis with their spins approximately in the plane perpendicular to the beam direction, the magnetic field can only rotate the spin distribution about its symmetry axis. There are therefore no observable perturbation effects prior to the detection of the first γ-ray. This can be seen from the formalism by substituting Eq. (24) into Eq. (12) and noting that $q = 0$ for these states. The observed perturbation is therefore due only to states between the two detected γ-ray transitions. Thus, if Eq. (29) is substituted into Eq. (18) and simplified, the result can be written

$$W = \sum_{kk_1k_2q\geqslant 0} B_{k_1}(I_1)A_k^{k_2k_1}(\delta_{\gamma_{12}}LL'I_2I_1) \times A_{k_2'}(\delta_{\gamma_{23}}LL'I_3I_2)\sqrt{(2k+1)}\left[\frac{2}{1+\delta_{q0}}\right] \times \begin{pmatrix} k_1 & k & k_2 \\ 0 & q & -q \end{pmatrix}\left[\frac{(k_2-q)!(k_1-q)!}{(k_2+q)!(k_1+q)!}\right]^{1/2} \times Q_k(E_{\gamma_{12}})Q_{k_2}(E_{\gamma_{23}})P_k^q(\cos\theta_1)P_{k_2}^q(\cos\theta_2) \times \frac{\cos[q(\phi_2-\phi_1-\Delta\theta_q)]}{\sqrt{1+(q\omega\tau)^2}} \quad (35)$$

where $P_k^q(\cos\theta)$ are Associated Legendre polynomials. This expression can be put in the form

$$W = \sum_{q\geqslant 0} b_q \frac{\cos[q(\Phi-\Delta\theta_q)]}{\sqrt{1+(q\omega\tau)^2}} \quad (36)$$

where $\Phi = \phi_2 - \phi_1$ and q is an integer between 0 and the maximum value of k. Note, however, that in general q takes both odd and even values, whereas only even terms are included in the similar formula for angular correlations and angular distributions. The odd terms disappear only when θ_1 or θ_2 is zero or a multiple of $\pi/2$. Since the anisotropy is also maximized when $\theta_1 = \theta_2 = \pi/2$, the ideal array for this geometry would have the detectors in the plane perpendicular to the beam, as in Ref. [18]. Eq. (35) is equivalent to the expressions given by Furuno [26].

Application of the magnetic field along the beam axis was advocated by the Chalk River group [25] and has been used by Alfter et al. [18] and Furuno et al. [19]. Both the 8π spectrometer [25] and the UTTAC array [19] have rings of detectors around the beam axis which, given the requirements for perturbed angular correlation measurements, virtually require that the field direction coincides with the beam axis.

Provided one is not interested in the precessions of states above the gating transitions, the only disadvantage of this geometry arises if one wishes to use the hyperfine fields within ferromagnetic foils, because then the target and foil must face the beam direction (at least approximately) with their thin dimension along the beam direction. It is difficult to magnetize thin foils perpendicular to the plane of the foil. In the measurements to date, Furuno et al. [19] have used an external field and no ferromagnetic host while Alfter et al. [18], used a superconducting magnet with a field of 4.5 T to ensure saturation of their ferromagnetic host foils.

3.3. Field perpendicular to the beam direction

The analysis of PDCO data becomes much more complex when the magnetic field is applied along any direction other than along the beam axis. However, due to the detector locations in the Australian National University CAESAR array, the case where the magnetic field is perpendicular to the beam direction, and the detectors are in the plane perpendicular to the field, is the one of primary interest to us. The CAESAR array can be configured with seven Compton suppressed Ge detectors in a vertical plane through the beam direction. The detector angles and numbering are shown in Table 1 and Fig. 3.

We define the 'beam-detector' frame to have the beam along the z-axis, the detectors in the x–z plane and the magnetic field along the y-axis. For the 'field' frame, we require the magnetic field along the z-axis, the beam along the x-axis and the detectors in the x–y plane. Thus the 'beam' frame

Table 1
Detector numbering and angles in the CAESAR array*

Number	θ°	ϕ°	Notes
1	144.5	0	
2	96.5	0	
3	48.0	0	
4	146.0	180	
5	98.0	180	
6	49.5	180	
7	0.0	0	a
8	45.0	90	b
9	45.0	270	b
10	135.0	90	b
11	135.0	270	b

*The angles θ and ϕ are in spherical polar coordinates with the z-axis along the beam and the x-axis (i.e. $\phi = 0$) vertically upwards.

[a] This detector is often removed to allow the beam to be dumped remotely.

[b] These detectors are to be installed in the near future.

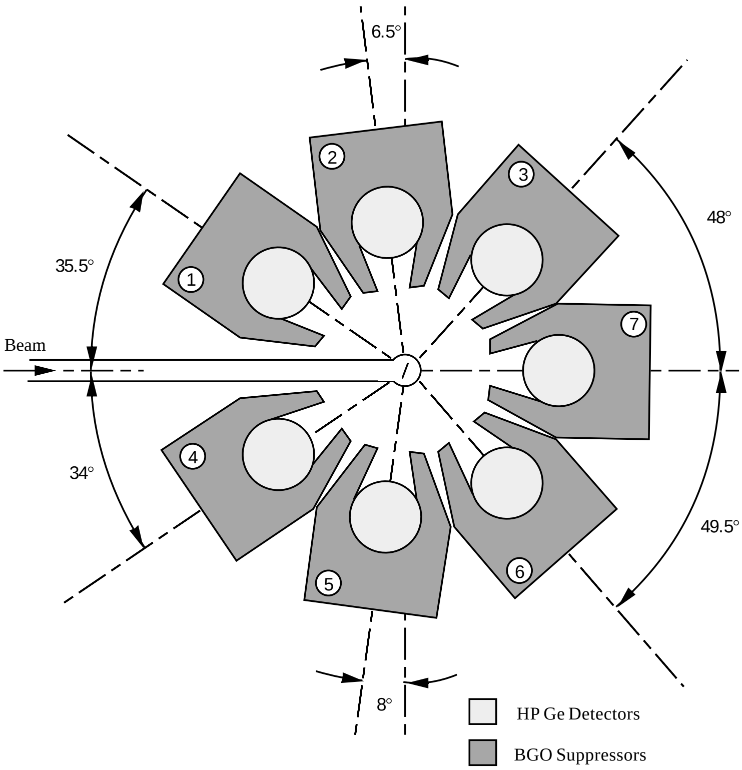

Fig. 3. Schematic of the CAESAR array showing the detector locations. The magnetic field is perpendicular to the plane of the detectors (i.e. into or out of the page).

is rotated into the 'field' frame by the Euler rotation $(\pi/2, \pi/2, \pi)$ and the perturbation factor for an integral magnetic perturbation in the 'beam' frame is

$$G_{kk'}^{qq'*} = \delta_{kk'} \sum_{Q} D_{qQ}^{k*}\left(\frac{\pi}{2}, \frac{\pi}{2}, \pi\right) \times \frac{\mathrm{e}^{\mathrm{i}Q\Delta\theta_Q}}{\sqrt{1+(Q\omega\tau)^2}} D_{q'Q}^{k}\left(\frac{\pi}{2}, \frac{\pi}{2}, \pi\right). \quad (37)$$

Unlike the situation considered in the previous subsection, the PDCO is now sensitive to the perturbations of all of the states involved in the cascade selected by the γ–γ coincidence as well as to the perturbations of the states which feed it from above. Because of this, we have found no useful simplified formula akin to Eq. (35) for the case where the magnetic field is perpendicular to the beam. In view of this greater complexity, it is of practical advantage to work with an array with a modest number of well positioned detectors.

Compared with the case where the field is applied along the beam direction, the main features and advantages of the perpendicular-field geometry are that (i) it is easy to magnetize thin target foils perpendicular to the beam, and (ii) information is obtained on the perturbations of states above the first detected γ-ray.

3.3.1. *CAESAR array*

We will begin to illustrate the effects of magnetic perturbations by considering the CAESAR array [35] in the configuration with which the first experiments were performed. The array is in the process of being upgraded [36] and the implications of this upgrade for PDCO measurements will be considered in Section 3.3.2.

To plan the first set of experiments, PDCOs were calculated for hypothetical cases to be observed with the CAESAR array [35] when configured with seven Compton-suppressed Ge detectors in the same plane as the beam and a magnetic field applied perpendicular to the detection plane. (See Table 1 and Fig. 3.) In the measurements, the direction of the magnetic field is reversed periodically. We refer to field 'up' when the field is along the positive y-axis in the 'beam' frame and use arrows, $\uparrow$ ($\downarrow$), to denote the field direction. Fig. 4 shows the calculated perturbed and unperturbed DCOs for a $4^+ \to 2^+ \to 0^+$ cascade with the initial alignment of the 4^+ state parametrized by a Gaussian distribution with $\sigma/I = 0.35$. This case is typical of any stretched E2 cascade. The $4^+ \to 2^+$ transition is registered at angle θ_1 while the $2^+ \to 0^+$ transition is detected at angle θ_2. In the CAESAR array ϕ_1 and ϕ_2 are either 0° or 180°, and the detectors are located at approximately 0°, $\pm 48^\circ$, $\pm 97^\circ$, and $\pm 145^\circ$ to the beam; hence the data for all two-detector combinations can be mapped onto four plots with $\theta_1 = 0^\circ$, 48°, 97° or 145° and $0 \leqslant \theta_2 \leqslant 180^\circ$. The PDCO in this case has the following symmetries

$$\begin{aligned} &W(\theta_1, \phi_1 = 0, \theta_2, \phi_2 = 0)\uparrow\downarrow \\ &\quad = W(\theta_1, \phi_1 = 0, \pi - \theta_2, \phi_2 = \pi)\uparrow\downarrow \\ &\quad = W(\theta_1, \phi_1 = \pi, \pi - \theta_2, \phi_2 = 0)\downarrow\uparrow \\ &\quad = W(\theta_1, \phi_1 = \pi, \theta_2, \phi_2 = \pi)\downarrow\uparrow. \end{aligned} \tag{38}$$

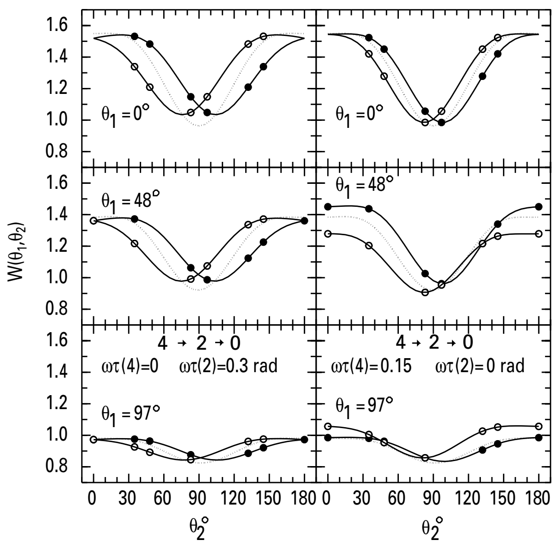

Fig. 4. Calculated unperturbed (dotted) and perturbed (solid) DCOs for a $4^+ \to 2^+ \to 0^+$ cascade observed with the CAESAR array. The left panels show a perturbation of the 2^+ state, while the right panels show a perturbation of the 4^+ state. The data points indicate the angles sampled by the array. Positive (negative) precession angles are denoted by solid (open) symbols. The case where $\theta_1 = 145^\circ$, which is intermediate between the 0° and 48° cases, is not shown.

The alignment of the 4^+ state due to the reaction (and unobserved γ-ray decays above the 4^+ state) is centered in the plane perpendicular to the beam axis. Since the observation of the $4^+ \to 2^+$ transition at angle θ_1 tends to select the alignment of the 2^+ state to be in the plane perpendicular to the direction of detection, the anisotropy of the DCO in the upper panel of Fig. 4 ($\theta_1 = 0^\circ$) is greater than that of an angular distribution with $\sigma/I = 0.35$. This mechanism also explains why the total intensity is reduced when $\theta_1 = 97^\circ$. The perturbation in the left-hand panels of Fig. 4 is due to a pure magnetic interaction in the 2^+ state alone with $\omega\tau = \pm 0.3$ mrad; the right-hand panels show the effect of a magnetic interaction in the 4^+ state alone for $\omega\tau = \pm 0.15$ mrad. The coincidence requirement eliminates side-feeding to the 2^+ state. While the perturbation of the intermediate state is manifested as a rotation of the radiation pattern combined with a small attenuation of the anisotropy, the perturbation of the upper state, when plotted in this way, is a more complex combination of rotation, attenuation and change in total intensity. It is clear that when $\theta_1 \neq 0$, the PDCOs are sensitive to the perturbation of the feeding state (e.g. 4^+) and the intermediate state (e.g. 2^+) in a different way.

There is a more intuitive way to understand these magnetic perturbations because they stem from rotations of the radiation pattern about the field direction: the precession of the 4^+ state behaves like an equal rotation of all detection angles in the array with respect to the beam direction, whereas the precession of the 2^+ level is manifest as a change in the effective angle between the detectors that detect the two γ-rays.

In general, neither the unperturbed nor the perturbed correlations shown in Fig. 4 can be written exactly in terms of the familiar sum of even

Legendre polynomials, $P_k(\cos\theta_2)$. For the CAESAR array it can be done exactly only when $\theta_1 = 0$.

Fig. 5 shows the influence of the alignment parameter σ/I on the PDCO. As σ/I increases, the orientation of the initial state diminishes and the DCO approaches the corresponding γ–γ angular correlation. It is clear from Fig. 5 that the anisotropy in the DCO is typically much greater than that in the corresponding angular correlation. The fact that the anisotropy is always very small when the first γ-ray is detected near 90° proves useful for checking the relative coincidence efficiencies of the detectors simultaneously with the DCO measurement [21].

3.3.2. Upgraded CAESAR array

The CAESAR array is to be upgraded to include an additional four high-efficiency Compton-suppressed detectors in the horizontal plane at angles $\pm 45°$ and $\pm 135°$ to the beam, as illustrated in Fig. 6 [36]. In the augmented array, we anticipate putting the magnetic field in the vertical direction, perpendicular to the plane of the new detectors and in the plane of the existing detectors. The detector at 0° may be removed. We again consider a $4^+ \to 2^+ \to 0^+$ coincidence event. There are now four types of PDCO to be considered:

(i) The $4^+ \to 2^+$ and $2^+ \to 0^+$ transitions are detected in the horizontal plane (Fig. 7). This case is very like that obtained for the present configuration of the array, except that all of the detectors are at equivalent angles with respect to the beam. It is therefore very sensitive to the perturbation, but has limited use to determine the alignment parameter σ/I.

(ii) The $4^+ \to 2^+$ and $2^+ \to 0^+$ transitions are detected in the vertical plane (Fig. 8). Since the detectors and the magnetic field are in the same plane, there is no difference in this case between the PDCO for the two field directions. These data are insensitive to the precessions but would be useful for determining σ/I.

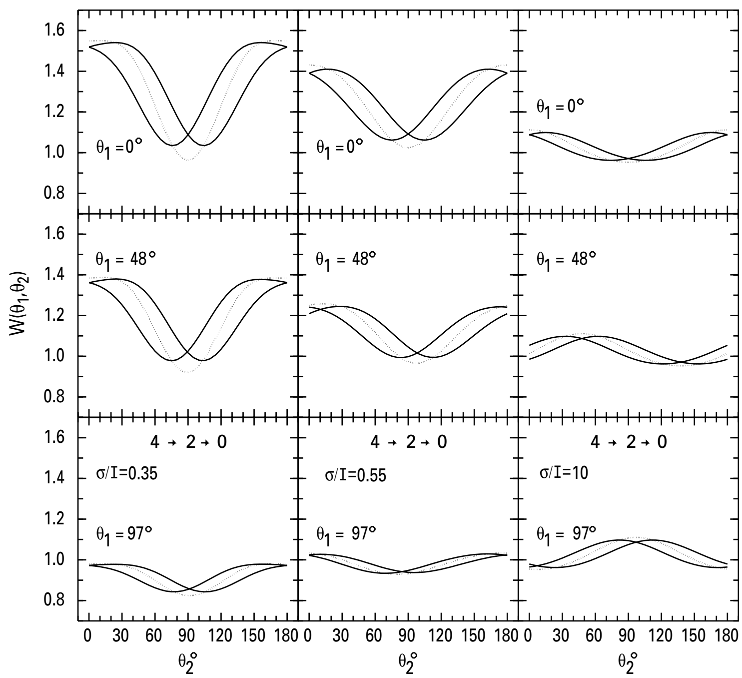

Fig. 5. Calculated unperturbed (dotted) and perturbed (solid) DCOs for a $4^+ \to 2^+ \to 0^+$ cascade observed with the CAESAR array showing the effect of varying the alignment parameter σ/I. In all panels $\omega\tau(2^+) = \pm 0.3$ rad. The panels in each column have the σ/I value indicated in the bottom panel.

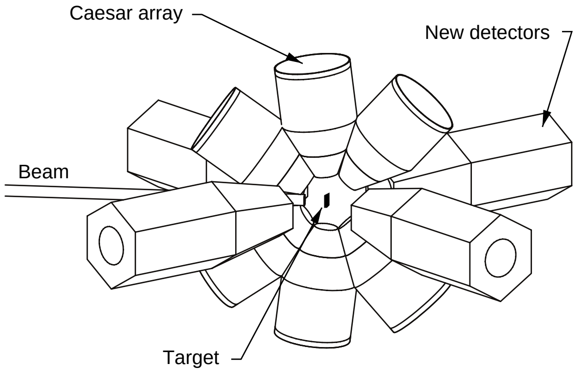

Fig. 6. Schematic of the upgraded CAESAR array. For PDCO measurements the magnetic field will be applied in the vertical direction, perpendicular to the plane of the new detectors.

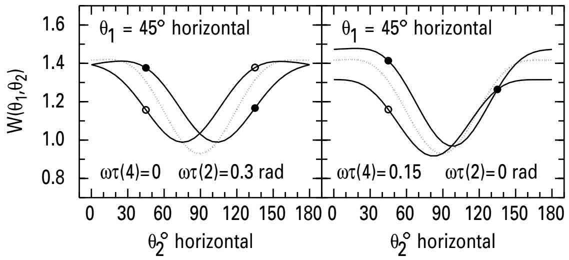

Fig. 7. PDCOs in upgraded CAESAR array with both transitions detected in the horizontal detectors. For further details see Fig. 4.

(iii) The $4^+ \rightarrow 2^+$ transition is detected in the vertical plane and the $2^+ \rightarrow 0^+$ transition is detected in the horizontal plane (Fig. 9). There is little difference between the perturbation of the 4^+ state and that of the 2^+ state for the same $\omega\tau$ values in this case. On their own, these data could therefore be open to misinterpretation, but in the context of the whole data set they give information about the total precession experienced by the nuclei in the cascade.

(iv) The $4^+ \rightarrow 2^+$ transition is detected in the horizontal plane and the $2^+ \rightarrow 0^+$ transition is detected in the vertical plane (Fig. 10). These data show a strong dependence on the magnitude of the 4^+ precession, but have no sensitivity to the change of field direction for 2^+ precessions. They are therefore very useful for determining the 4^+ precession.

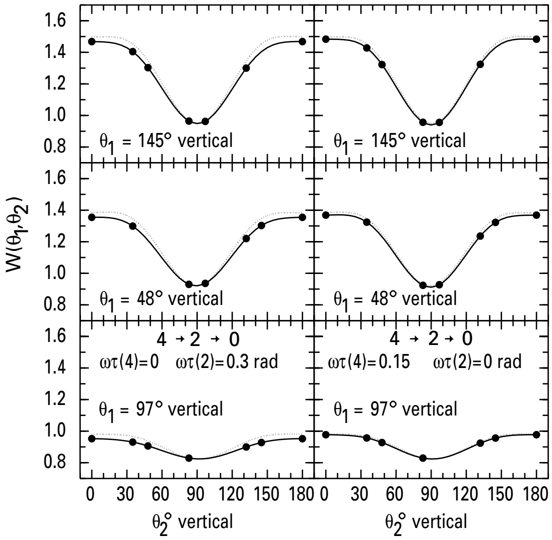

Fig. 8. PDCOs in upgraded CAESAR array with both transitions detected in the vertical detectors. For further details see Fig. 4. These data are not sensitive to the field direction.

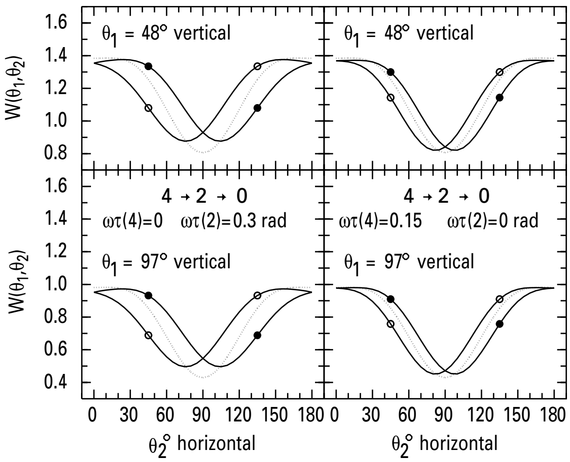

Fig. 9. PDCOs in upgraded CAESAR array with the $4^+ \rightarrow 2^+$ transition detected in the vertical plane while the $2^+ \rightarrow 0^+$ transition is detected in the horizontal plane. For further details see Fig. 4. There is little difference between the PDCOs for 2^+ (left panels) and 4^+ (right panels) precessions of the same magnitude.

Thus the whole data set is of value in characterizing the PDCO and extracting the quantities of interest, especially if it is analyzed using a global fit.

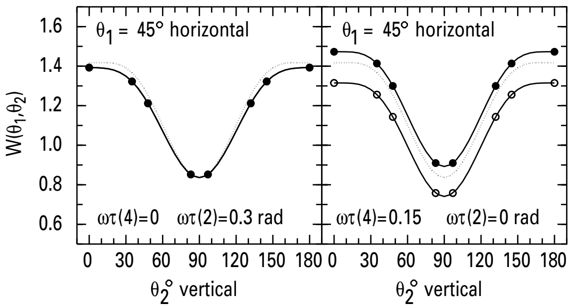

Fig. 10. PDCOs in upgraded CAESAR array with the $4^+ \rightarrow 2^+$ transition detected in the horizontal plane while the $2^+ \rightarrow 0^+$ transition is detected in the vertical plane. For further details see Fig. 4. There is no change due to the 2^+ precession when the magnetic field direction is reversed, whereas the 4^+ precession results in a considerable effect.

4. Summary and concluding comments

In summary, we have set down the formalism required to calculate perturbed directional correlations from reaction-oriented nuclei (PDCO), and have applied them to examine the characteristics of magnetic perturbations in the CAESAR array, both in its present incarnation and its future upgrade. The case of combined electric and magnetic interactions is of considerable interest to us, but since it introduces further complications, and destroys some of the symmetries present in the pure magnetic case, we discuss it separately [20].

In most γ-ray spectroscopy experiments, the data for a number of detector pairs would be summed; however, in general, this cannot be done for PDCO measurements without the loss of information on the perturbation. For this reason, we have considered γ–γ coincidences between individual detector pairs only. In some cases it might be necessary, on practical grounds, to sum the coincidence data for several detector pairs. If this is done, the data can still be analyzed rigorously by computing the sum of individual two-detector PDCOs that corresponds to the experimental data. Furthermore, any approximations used to analyze PDCO data in a large array can be assessed rigorously by employing the procedures described here.

The applications of the formalism to the analysis of experimental data are described in an accompanying paper [21].

Acknowledgements

We thank our colleagues in the Nuclear Spectroscopy Group for their interest and support. We are particularly grateful to Dr A.P. Byrne for providing Fig. 6.

References

[1] K.S. Krane, R.M. Steffen, R.M. Wheeler, Nucl. Data Tables 11 (1973) 351.

[2] A. Krämer-Flecken, T. Morek, R.M. Lieder, W. Gast, G. Hebbinghaus, H.M. Jäger, W. Urban, Nucl. Instr. and Meth. A 275 (1989) 333.

[3] L.P. Ekström, A. Nordlund, Nucl. Instr. and Meth. A 313 (1992) 421.

[4] A. Nordlund, Nucl. Instr. and Meth. A 368 (1996) 731.

[5] I. Wiedenhöver, O. Vogel, H. Klein, A. Dewald, P. von Brentano, J. Gableske, R. Krücken, N. Nicolay, A. Gelberg, P. Petkov, A. Gizon, J. Gizon, D. Bazzacco, C. Rossi Alvarez, G. de Angelis, S. Lunadi, P. Pavan, D.R. Napoli, S. Frauendorf, F. Dönau, R.V.F. Janssens, M.P. Carpenter, Phys. Rev. C 58 (1998) 721.

[6] E. Karlsson, E. Matthias, K. Siegbahn, Perturbed Angular Correlations, North-Holland, Amsterdam, 1964.

[7] W.D. Hamiltion, The Electromagnetic Interaction in Nuclear Spectroscopy, North-Holland, Amsterdam, 1975.

[8] H. Morinaga, T. Yamazaki, In-Beam Gamma-Ray Spectroscopy, North-Holland, Amsterdam, 1976.

[9] J. Christiansen, Hyperfine Interactions in Radioactive Nuclei, Springer, Berlin, 1983.

[10] A.E. Stuchbery, S.S. Anderssen, A.P. Byrne, P.M. Davidson, G.D. Dracoulis, G.J. Lane, Phys. Rev. Lett. 76 (1996) 2246.

[11] F. Brandolini, N.H. Medina, A.E. Stuchbery, S.S. Anderssen, H.H. Bolotin, D. Bazzacco, D. De Acuña, M. De Poli, R. Menegazzo, P. Pavan, C. Rossi Alvarez, G. Vedovato, Eur. Phys. J. A 3 (1998) 129.

[12] R.H. Mayer, G. Kumbartzki, L. Weissman, N. Benczer-Koller, C. Broude, J.A. Cizewski, M. Hass, J. Holden, R.V.F. Janssens, T. Lauritsen, I.Y. Lee, A.O. Macchiavelli, D.P. McNabb, M. Satteson, Phys. Rev. C 58 (1998) R2640.

[13] L. Weissman, R.H. Mayer, G. Kumbartzki, N. Benczer-Koller, C. Broude, J.A. Cizewski, M. Hass, J. Holden, R.V.F. Janssens, T. Lauritsen, I.Y. Lee, A.O. Macchiavelli, D.P. McNabb, M. Satteson, Phys. Lett. B 446 (1999) 22.

[14] U. Birkental, A.P. Byrne, S. Heppner, H. Hübel, W. Schmitz, P. Fallon, P.D. Forsyth, J.W. Roberts, H. Kluge, E. Lubkiewicz, G. Goldring, Nucl. Phys. A 555 (1993) 643.
[15] A. Jungklaus, C. Teich, V. Fischer, D. Kast, K.P. Lieb, C. Lingk, C. Ender, T. Härtlein, F. Köck, D. Schwalm, J. Billowes, J. Eberth, H.G. Thomas, Phys. Rev. Lett. 80 (1998) 2793.
[16] C. Teich, A. Jungclaus, V. Fischer, D. Kast, K.P. Lieb, C. Lingk, C. Ender, T. Härtlein, F. Köck, D. Schwalm, J. Billowes, J. Eberth, H.G. Thomas, Phys. Rev. C 59 (1999) 1943.
[17] L. Weissman, M. Hass, N. Benczer-Koller, C. Broude, G. Kumbartzki, Nucl. Instr. and Meth. Phys. Res. A 416 (1998) 351.
[18] I. Alfter, E. Bodenstedt, W. Knichel, J. Schüth, Z. Phys. A 357 (1997) 13.
[19] K. Furuno, T. Jumastu, Y. Sasaki, K. Yamada, M. Ozaki, Y. Tutsui, T. Komatsubara, Annual Report 1999, University of Tsukuba Tandem Accelerator Center, UTTAC-68, 2000, p. 39.
[20] A.E. Stuchbery, M.P. Robinson, in preparation.
[21] M.P. Robinson, A.E. Stuchbery, Nucl. Instr. and Meth. A (2002) in press.
[22] M.P. Robinson, A.E. Stuchbery, R.A. Bark, A.P. Byrne, G.D. Dracoulis, S.M.Mullins, A.M. Baxter, in preparation.
[23] K. Alder, A. Winther, Electromagnetic Excitation, North-Holland, Amsterdam, 1975.
[24] T. Yamazaki, Nucl. Data A 3 (1967) 1.
[25] D. Ward, H.R. Andrews, J.S. Geiger, AECL report TASCC-1-19-07, 1984; D. Ward, J.S. Geiger, H.R. Andrews, AECL report TASCC-1-19-08, 1984.
[26] K. Furuno, Annual Report 1998, University of Tsukuba Tandem Accelerator Center, UTTAC-67, 1999, p. 37.
[27] M.P. Carpenter, C.R. Bingham, L.H. Courtney, V.P. Janzen, A.J. Larabee, Z.-M. Liu, L.L. Riedinger, W. Schmitz, R. Bengtsson, T. Bengtsson, W. Nazarewicz, J.-Y. Zhang, J.K. Johansson, D.G. Popescu, J.C. Waddington, C. Baktash, M.L. Halbert, N.R. Johnson, I.Y. Lee, Y.S. Schutz, J. Nyberg, A. Johnson, R. Wyss, J. Dubuc, G. Kajrys, S. Monaro, S. Pilotte, K. Honkanen, D.G. Sarantites, D.R. Haenni, Nucl. Phys. A 513 (1990) 125.
[28] M.J.L. Yates, in: K. Siegbahn (Ed.), Alpha-, Beta-, and Gamma-Ray Spectroscopy, Vol. 2, North-Holland, Amsterdam, 1965, p. 1691.
[29] D.C. Camp, A.L. Van Lehn, Nucl. Instr. and Meth. 76 (1969) 192.
[30] K.S. Krane, Nucl. Instr. and Meth. 109 (1973) 401.
[31] A.E. Stuchbery, Nucl. Instr. and Meth. A 385 (1997) 547.
[32] N. Benczer-Koller, M. Hass, J. Sak, Ann. Rev. Nucl. Part. Sci. 30 (1980) 53.
[33] K. Alder, E. Matthias, W. Schneider, R.M. Steffen, Phys. Rev. 129 (1963) 1199.
[34] E. Matthias, W. Schneider, R.M. Steffen, Phys. Rev. 125 (1962) 261.
[35] G.D. Dracoulis, A.P. Byrne, Department of Nuclear Physics Annual Report, Australian National University, ANU-P/1052, p.115, 1989, Unpublished.
[36] G.D. Dracoulis R.A. Bark, A.P. Byrne, Department of Nuclear Physics Annual Report, Australian National University, ANU-P/1420, p. 126, 1999, unpublished.